9. R. B. McKibben and J. A. Simpson, *ibid.*, p. 3545.
10. R. W. Fillius and C. E. McIlwain, *ibid.*, p. 3589; T. G. Northrop, C. K. Goertz, M. F. Thomsen, *ibid.*, p. 3579.
11. The magnetic shell parameter L identifies the drift shell of a trapped particle and is defined for a dipole field as $L = R/\cos^2 \lambda$, where R is the radial distance from the dipole center and λ is the magnetic latitude. At the magnetic equator, therefore, $L = R$.
12. E. J. Smith, personal communication.
13. B. J. Teegarden, F. B. McDonald, J. H. Trainor, W. R. Webber, E. C. Roelof, *J. Geophys. Res.* **79**, 3615 (1974).
14. M. H. Acuña and N. F. Ness, *Nature (Lond.)* **253**, 327 (1975); personal communication.
15. J. H. Wolfe, J. D. Mihalov, H. R. Collard, D. D. McKibbin, L. A. Frank, D. S. Intriligator, *J. Geophys. Res.* **79**, 3489 (1974).
16. The synodic rotation period (relative to the Sun-Jupiter line) is adopted because the primary factor breaking cylindrical symmetry about Jupiter's rotation axis is the solar wind pressure. Therefore, phenomena that are likely to depend on the interaction of Jupiter's dipole magnetic field with the solar wind, such as the release of energetic electrons from the magnetosphere, should exhibit the synodic period. System III is defined in *Information Bulletin 8* (International Astronomical Union, Utrecht, Netherlands, March 1962) and is discussed by G. D. Mead [*J. Geophys. Res.* **79**, 3514 (1974)].
17. We are especially grateful for the exceptional assistance of those associated with the Pioneer Project Office, including C. F. Hall, A. Wilhelmi, J. Lepetich, R. Fimmel, and A. Natwick. Our experiment was fabricated and prepared for space flight in the Laboratory for Astrophysics and Space Research of the Enrico Fermi Institute for which we thank the staff, particularly R. M. Jacquet and J. E. Lamport. We thank W. D. Schroeder and C. W. Barnes who assisted in the data-processing. In the analysis of the Pioneer 11 data we benefited from the assistance of T. F. Conlon and D. L. Chenette, especially in determining the phase of the variations between Pioneer 10 and Pioneer 11. This work was supported in part by NASA contract NAS 2-5601 and NAS 2-6551 with the Ames Research Center, NASA grant NGL 14-001-006, and NSF grant GA-38913X.

14 March 1975

Pioneer 11 Observations of Energetic Particles in the Jovian Magnetosphere

Abstract. *Knowledge of the positional distributions, absolute intensities, energy spectra, and angular distributions of energetic electrons and protons in the Jovian magnetosphere has been considerably advanced by the planetary flyby of Pioneer 11 in November–December 1974 along a quite different trajectory from that of Pioneer 10 a year earlier. (i) The previously reported magnetodisc is shown to be blunted and much more extended in latitude on the sunward side than on the dawn side. (ii) Rigid corotation of the population of protons* $E_p \approx 1$ *million electron volts in the magnetodisc is confirmed. (iii) Angular distributions of energetic electrons* $E_e > 21$ *million electron volts in the inner magnetosphere are shown to be compatible with the Kennel-Petschek whistler-mode instability. (iv) A diverse body of magnetospheric effects by the Jovian satellites is found. (v) Observations of energetic electrons in to a radial distance of 1.59 Jovian radii provide a fresh basis for the interpretation of decimetric radio noise emission.*

A second body of in situ observations of the Jovian magnetosphere was obtained by instruments on the Pioneer 11 spacecraft of the Ames Research Center of the National Aeronautics and Space Adminstration during November–December 1974. Results of the predecessor mission of Pioneer 10, which flew by Jupiter 1 year earlier, have been reported in the 25 January 1974 issue of *Science* and in the 1 September 1974 issue of the *Journal of Geophysical Research.*

We present here a preliminary report of observations of energetic electrons and protons with the University of Iowa instrument on Pioneer 11.

The hyperbolic encounter trajectory of Pioneer 10 with Jupiter was prograde in a plane inclined 13.8° to the planet's equatorial plane and had periapsis at a radial distance of 2.85 R_J (1 R_J = 71,372 km, the adopted value of the equatorial radius of the planet). The encounter trajectory of Pioneer 11 was retrograde in a plane inclined at 51.8° and had periapsis at a radial distance of 1.60 R_J (Fig. 1). Thus the new observations spanned a considerably greater range of latitude and longitude; extended inward much closer to the planet; and were obtained, of course, at a different epoch.

Pioneer 11 passed through periapsis at 0603 ERT (Earth received time) on DOY (day of the year) 337/1974 (3 December 1974). Relative to a plane containing the Sun and the poles of the ecliptic plane, the local time of the spacecraft at a radial distance r of 100 R_J was 9.2 hours inbound and 11.6 hours outbound. The spacecraft crossed the reference plane of the sunward side of the planet at 0025 ERT/DOY 339 at a radial distance of 36.4 R_J.

The spin period of Pioneer 11 was 11.89 seconds during Jovian encounter, and, as with Pioneer 10, the spin axis was pointed continuously at Earth to an accuracy of better than 1°.

Our instrument on Pioneer 11 was considerably improved over that on Pioneer 10 by the replacement of one of the original Geiger-Müller tube detectors with a thin (29-μm) single-element, solid-state detector for unambiguous detection of protons $0.61 < E_p < 3.41$ Mev and by modification of another detector so as to increase our sensitivity to low-energy electrons by increasing the geometric factor fourfold and by lowering the detection threshold from 60 to 40 kev. General characteristics of the instrument and other experimental details have been described in detail by Van Allen *et al.* (*1*).

The first crossing of the bow shock was identified by the magnetometer and plasma analyzer experimenters at 109.7 R_J on DOY 330 (26 November 1974) at 0420 ± 05 ERT. After this event there were a miscellany of magnetopause and bow shock crossings until a "final" durable crossing of the magnetopause at about 65 R_J on DOY 333 at 1345 ERT. Particle intensities on the inbound traversal of the magnetodisc were generally similar to those

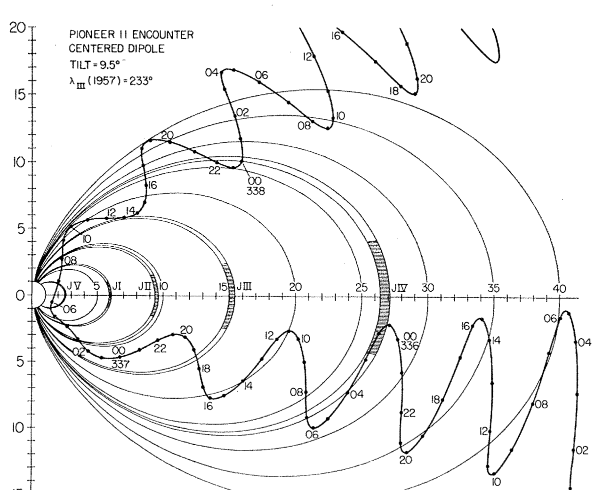

Fig. 1. Trace of the Jovian encounter trajectory of Pioneer 11 on a magnetic meridian plane for the centered dipole model of Randall [see (*1*)] updated to December 1974. Cross-hatched regions are those swept out by satellites JI through JV. The unit of distance is the equatorial radius of Jupiter, 71,372 km.

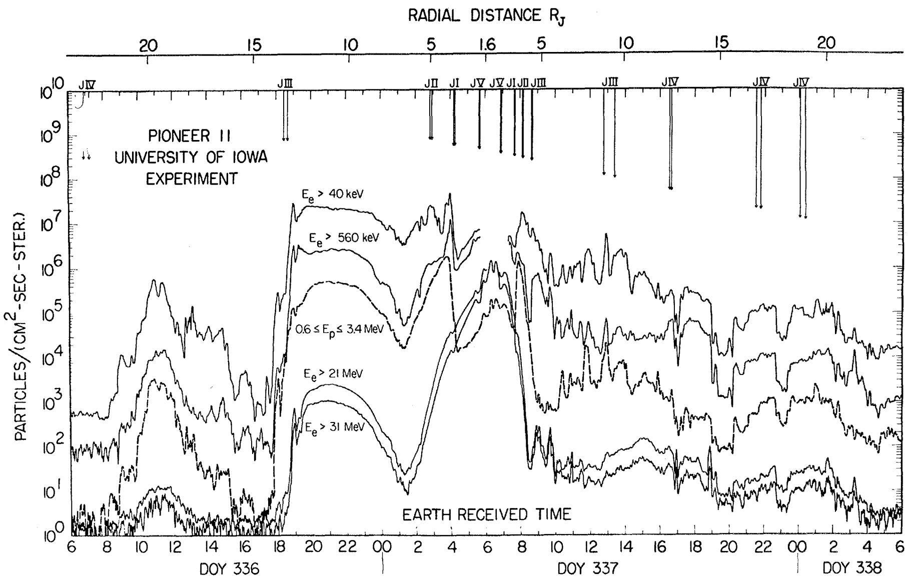

Fig. 2. Absolute, spin-averaged unidirectional intensities of electrons in several energy ranges as labeled and protons $0.61 \leq E_p \leq 3.41$ Mev as a function of time during traversal of the central magnetosphere. Arrows in upper part of the diagram show traversal of magnetic shells through satellites as derived from Fig. 1.

observed on the Pioneer 10 mission and again showed a 10-hour periodicity corresponding to the wobbling magnetodisc model. In detail, however, the observations differed markedly from those of Pioneer 10, thus emphasizing the strong temporal variability of the outer magnetosphere. Data on the outbound traversal of the outer magnetosphere near the noon meridian at high latitudes (Fig. 1) demonstrated conclusively that the sunward magnetodisc is blunted and much thickened in latitude in contrast to its relative thinness in latitude near the dawn meridian (Pioneer 10).

From the magnetopause at R_J inward to at least 30 R_J, protons $0.61 \leq E_p \leq 3.41$ Mev exhibit corotational streaming, as revealed by Fourier analysis of the angular distribution data with an equation of the form

$$f(\varphi) = M\,[1 + K \cos(\varphi - \Delta)]$$

with the roll angle of the detector's axis φ measured from the ascending node of the spacecraft's equator on the ecliptic. The phase angle Δ is about 180°, and K is approximately a linear function of radial distance r with a value of 0.32 at $r = 65$ R_J. These findings correspond to corotational streaming of protons $E_p \approx 1$ Mev with a spectral index $\gamma \approx 1.8$ in a differential energy spectrum of power law form, the index being approximately independent of r over the range $65 > r > 30$ R_J. This result confirms the Pioneer 10 observations of Trainor *et al.* (*2*).

The spin-averaged unidirectional intensities of electrons in several energy ranges as labeled and of protons $0.61 < E_p < 3.41$ Mev are shown in Fig. 2 as a function of time during traversal of the central magnetosphere. The great complexity of the curves presumably results from a combination of effects: (i) the geometric nature of the trajectory as shown in Fig. 1; (ii) satellite sweeping effects; (iii) the changing angle between the spin axis of the spacecraft and the local magnetic vector; (iv) the likely nondipolar nature of the close-in magnetic field; (v) the effects of plasma instabilities, both spontaneous and induced by the motion of the several satellites through the magnetospheric plasma; (vi) large-scale electric fields induced by fluctuating solar wind pressure; and perhaps (vii) other effects, such as instabilities in ionosphere-magnetosphere coupling. Each of these matters is the subject of further study.

In our paper on Pioneer 10 results (*1*), we gave tentative results on the intensities of low-energy electrons interior to the magnetic shell of Io and described the difficulties of assuring their validity. The problems have been alleviated by our Pioneer 11 results, mainly because of the considerably enhanced sensitivity of the modified electron detector (see above). In Fig. 2, we have omitted portions of the curves for $E_e > 40$ kev and $E_e > 560$ kev near periapsis, pending fuller analysis. However, it is already reasonably certain that our earlier, tentative intensities of these components were too great by as much as a factor of 10. Hence, we no longer have a serious

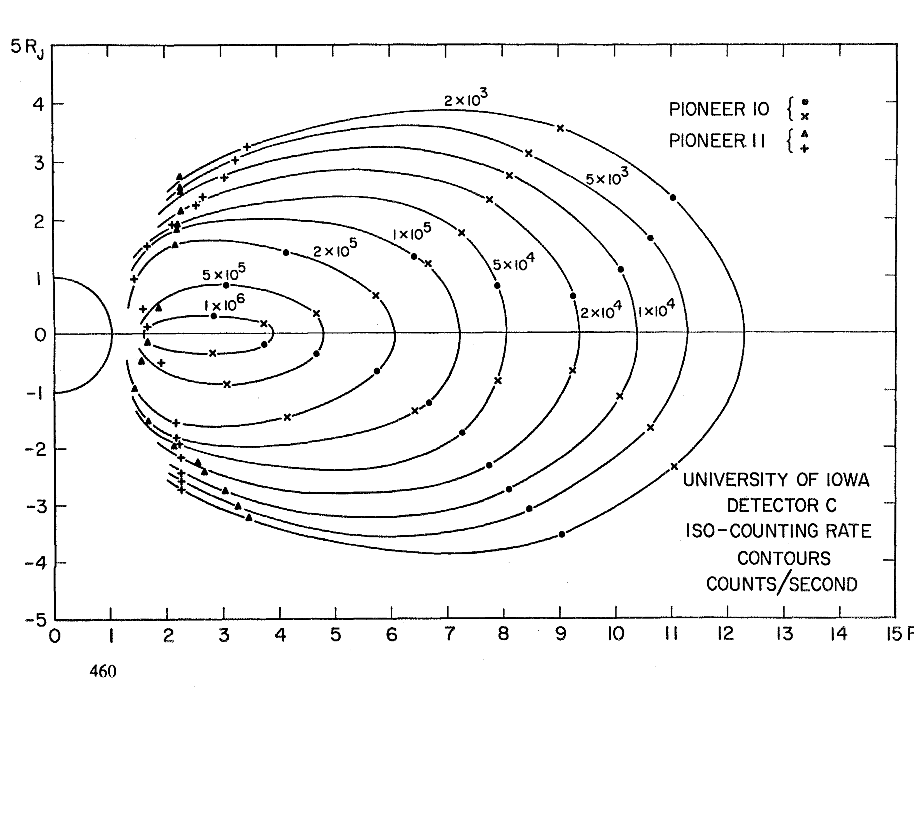

Fig. 3. Iso-counting rate contours for energetic electron detector C. Omnidirectional intensities of electrons $E_e > 21$ Mev are found by multiplying the counting rate by 23. This figure shows combined observations from the Pioneer 10 and Pioneer 11 missions based on the use of a centered dipole model with a tilt of 9.5° toward system III longitudes of 230° and 233°, respectively. Circles and triangles are observed points for Pioneer 10 and Pioneer 11, respectively; times signs and plus signs are corresponding reflections in the magnetic equatorial plane.

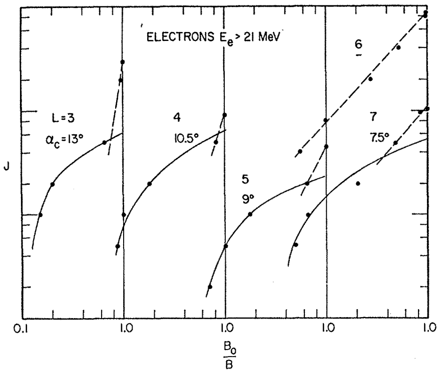

Fig. 4. Dependence of the omnidirectional intensity of electrons $E_e > 21$ Mev on (B_0/B) as derived from Fig. 3. The circles are the observed points; solid lines are according to the Kennel-Petschek theory of whistler-mode, pitch-angle scattering. The vertical scale is arbitrary and different for each set of data (see text).

disagreement with the intensities reported by Fillius and McIlwain (*3*) for similar energy ranges.

The intensities of electrons $E_e > 21$ Mev and $E_e > 31$ Mev are relatively smooth functions of time. In Fig. 3 are shown iso-counting rate contours in a magnetic meridian plane, based on both Pioneer 10 and Pioneer 11 observations with nominally identical detectors ($E_e >$ 21 Mev). In one region of approximate overlap of the respective trajectories, the counting rates of the two detectors agree to within 20 percent or better. An equatorial profile of absolute intensities of electrons derived from Fig. 3 shows a clear maximum with omnidirectional intensity $J = 3.8 \times 10^7$ (cm^2 sec)$^{-1}$ at $r = 2.5\ R_J$. Also from Fig. 3 we have derived values of J versus (B_0/B) at constant L values, where B is the local scalar value of the magnetic field and B_0 is its equatorial value on the same dipolar magnetic shell specified by the McIlwain parameter L (Fig. 4). A preliminary interpretation of these results in terms of resonance interaction between whistler-mode noise and high-energy electrons is as follows. Kennel and Petschek (*4*) show that magnetospheric electrons with energies above a critical energy

$$E_c = B^2/[8\pi NA(1 + A)^2]$$

are pitch angle–scattered by whistler noise [for definitions of these quantities, see Kennel and Petschek (*4*)]. Electrons with energies below E_c are not affected by this mode. Using the magnetic field values of Smith *et al.* (*5*) and the plasma number densities N determined by Frank *et al.* (*6*), we find that $B^2/8\pi N$ is 11 Mev at $L = 3$. In the inner magnetosphere it is probable that weak pitch-angle diffusion prevails. Then the anisotropy factor A is of the order of 0.2, and E_c at $L = 3$ is 38 Mev and thus above the threshold of detector C. This detector will thus count particles that are unaffected by the whistler noise (21 Mev $< E < E_c$) as well as particles that are affected ($E > E_c$). For particle energies above E_c the equilibrium pitch-angle (α) distribution at the equator was predicted by Kennel and Petschek as

$$j\ (E > E_c) \approx \ln\left(\frac{\sin \alpha}{\sin \alpha_c}\right)$$

where α_c is the loss cone angle at the equator. The adiabatic pitch angle transformation allows us to calculate the unidirectional intensity j and hence the omnidirectional intensity $J\ (E > E_c)$ as a function of (B_0/B) along a particular field line, treating α_c as a free parameter whose value is chosen for best agreement with the observations. The resulting calculations for several values of L are shown as solid lines in Fig. 4. The circles are the observed values on an arbitrary scale of intensity, different for each L. The agreement is satisfactory for $(B_0/B) \lesssim 0.6$. For $(B_0/B) > 0.6$ the observed values of J increase much more rapidly with (B_0/B). These rapid increases (dashed curves in Fig. 4) are consistent with pancake distributions at the equator of the form $j \approx \sin^m\alpha$. We attribute these dashed portions of the curves to particles with energies below E_c which are unaffected by the whistler noise. The complete set of data points is consistent with an equatorial distribution of the form

$$J = A(E) \sin^m \alpha + B(E) \ln\left(\frac{\sin \alpha}{\sin \alpha_c}\right)$$

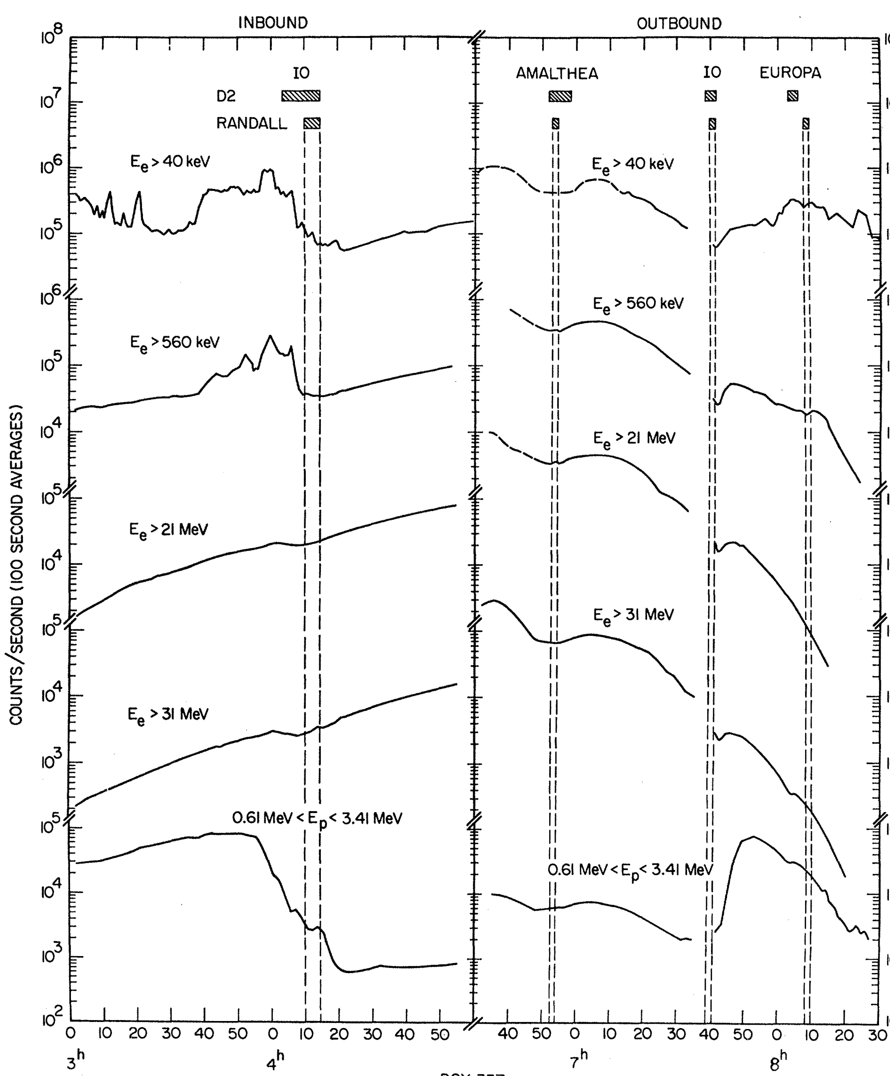

Fig. 5. Effects of Io and Amalthea on particle intensities.

with $A(E) = 0$ for $E > E_e$ and $B(E) = 0$ for $E < E_e$. Values of m for low L values are 6 to 10. The observed data exhibit a smoothly changing character from $L = 2$ to $L = 10$ with the noteworthy exception of $L = 6$ (Fig. 4). The more isotropic component of the angular distribution is absent at $L = 6$. It is tempting to associate this anomaly with the satellite Io (JI). Io can conceivably inhibit the development of whistler waves in a number of different ways.

Among the various satellite effects that can be identified in the Pioneer 10 and Pioneer 11 data, the most clear-cut and dramatic effect is that caused by Io as shown in Fig. 2 and in larger scale in Fig. 5. The intensities of protons $0.61 \leq E_p \leq 3.41$ Mev are reduced by a factor of about 100 interior to Io's magnetic shell and the intensities of electrons $E_e > 40$ kev and > 560 kev are reduced by a factor of about 10 (inbound), whereas the intensities of electrons $E_e > 21$ and > 31 Mev are only slightly affected.

Full analysis of satellite effects is the most promising technique for understanding the physical dynamics of the magnetosphere of Jupiter, a technique that is not available for the magnetosphere of Earth.

J. A. VAN ALLEN
B. A. RANDALL
D. N. BAKER
C. K. GOERTZ
D. D. SENTMAN
M. F. THOMSEN
H. R. FLINDT
Department of Physics and Astronomy, University of Iowa, Iowa City 52242

References and Notes

1. J. A. Van Allen, D. N. Baker, B. A. Randall, D. D. Sentman, *J. Geophys. Res.* **79**, 3559 (1974).
2. J. H. Trainor, F. B. McDonald, B. J. Teegarden, W. R. Webber, E. C. Roelof, *ibid.*, p. 3600.
3. R. W. Fillius and C. E. McIlwain, *ibid.*, p. 3589.
4. C. F. Kennel and H. E. Petschek, *ibid.* **71**, 1 (1966).
5. E. J. Smith, L. Davis, Jr., D. E. Jones, P. J. Coleman, Jr., D. S. Colburn, P. Dyal, C. P. Sonett, A. M. A. Frandsen, *ibid.* **79**, 3501 (1974).
6. L. A. Frank, K. L. Ackerson, J. H. Wolfe, J. D. Mihalov, *Univ. Iowa Res. Rep. 75-5* (January 1975).
7. The work has been supported in large part by contracts NAS2-5603 and NAS2-6553 with the Ames Research Center (ARC) of the National Aeronautics and Space Administration and by contract N00014-68-A-0196-0009 with the Office of Naval Research. We thank in particular C. F. Hall and his Pioneer Project staff at the ARC, and R. F. Randall of the University of Iowa, who designed and developed the electronics of the University of Iowa experiment and supervised and conducted all engineering aspects of the construction and preflight testing and integration into the spacecraft.

Jovian Protons and Electrons: Pioneer 11

We present here a preliminary account of the Pioneer 11 passage through the Jovian magnetosphere as viewed by the particle detector systems of the Goddard Space Flight Center and the University of New Hampshire. The detector systems and their operation have been described elsewhere (*1, 2*). In this report we will restrict our comments almost entirely to the region well within the Jovian magnetosphere, using data from the low energy telescope (LET-II). This detector system measures the proton flux from 0.2 to 21.2 Mev in seven energy intervals and the electron flux from 0.1 to 2 Mev in four intervals. It is well shielded, has a small geometric factor (0.015 cm^2-ster), and has an extended dynamic range allowing flux measurements to $\sim 3 \times 10^7$ cm^{-2} sec^{-1}. Representative electron and proton rates (up to ~ 2 Mev) are sampled over eight angular sectors to study particle anisotropies.

In an earlier Pioneer 10 paper (*2*) we described the Jovian magnetosphere in terms of certain characteristic regions: the region outside the magnetosphere where large fluxes of Mev electrons and protons are observed to be coming from the magnetosphere; the outer Jovian magnetosphere extending from bow shock crossings to $\sim$ 50 Jupiter radii (R_J), a region of quasi-trapping and diffusion; a transition region between $\sim$ 50 and $\sim$ 25 R_J, for example, between the outer diffusion zone and the region where the magnetic field rigidly rotates with the planet; and the region inside ~ 25 R_J, which is the really stable trapping region. This is a tentative morphology and is similar to that advanced by the other Pioneer 10 particle experimenters (*3*). The topology of this magnetosphere which emerges from the results of the particle, magnetic field (*4*), and plasma (*5*) measurements is very complicated: it consists of a rapidly rotating, giant magnetosphere which is easily deformed, where the physics is often dominated by a hot plasma inferred but not directly measured by Pioneer; the offset and tilted magnetic field results in a complicated, floppy motion of the magnetic field and the particles within it; and Pioneer 10 results showed quite a different character for this magnetosphere inbound on the sun side, as opposed to the outbound trajectory near the dawn meridian where the electrons and protons were much more concentrated near the equator.

On Pioneer 10, increases of low-energy Jovian electrons (0.2 to 8 Mev) were observed more than 1 astronomical unit (A.U.) away from Jupiter (*6*). On Pioneer 11 these increases were first observed in January 1974, when the spacecraft was ~ 2 A.U. from the planet. These electron increases persisted over $\gtrsim 5$-day periods and tended to recur at 27-day intervals. Furthermore, during the first half of 1974, many of these electron increases were readily detected at 1 A.U. by a more sensitive detector on Interplanetary Monitoring Platform 7. Because of space limitations, these observations will be presented elsewhere. They further

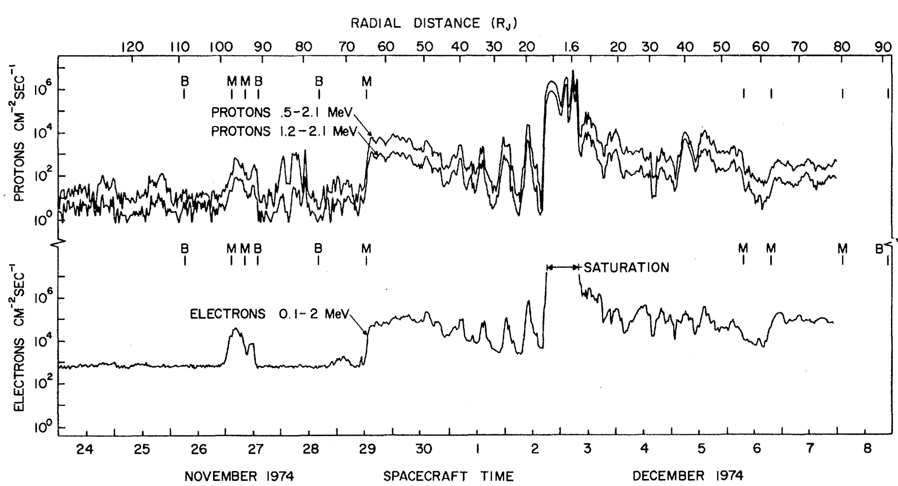

Fig. 1. Fluxes are shown for protons (0.5 to 2.1 Mev and 1.2 to 2.1 Mev) and electrons (0.1 to 2 Mev) for the period 24 November to 8 December 1974. The locations of crossing of the bow shock (B) and magnetopause (M) are noted (*12*). The relatively high background in this electron measurement from the LET-II telescope amounts to ~ 2 count sec^{-1} and is due to gamma rays from the radioisotope power supply.